Ligand Effects in Platinum Binding to DNA. A Comparison of DNA Binding Properties for *cis*- and *trans*-[$PtCl_2$(amine)$_2$] (amine = NH_3, pyridine)†

Y. Zou,‡ B. Van Houten,§,⊥ and N. Farrell*,‡,⊥

Departments of Chemistry and of Pathology and The Vermont Cancer Center, The University of Vermont, Burlington, Vermont 05405

Received March 1, 1993; Revised Manuscript Received June 2, 1993®

ABSTRACT: The DNA binding properties of *cis*- and *trans*-[$PtCl_2$(pyridine)$_2$] have been examined and compared with their NH_3 analogs, *cis*- and *trans*-DDP. The presence of a planar ligand reduces the rates of DNA binding but does not greatly affect the overall conformation of CT DNA, as measured by circular dichroism spectroscopy. The sequence specificity of *trans*-[$PtCl_2$(py)$_2$] includes alternating purine–pyrimidine sequences. The sequence specificity is further different between the two pyridine isomers, and the steric effects of two *cis*-pyridine groups are demonstrated by the appearance of relatively few binding sites in the 49-bp duplex. The effects of the pyridine ligand are further manifested by a greatly enhanced DNA–DNA interstrand cross-linking efficiency for the trans isomer, with a cross-link per adduct frequency of between 0.14 and 0.23, depending on the r_b of the sample. The unwinding of closed circular pUC19 DNA by *trans*-[$PtCl_2$(pyridine)$_2$] is also more efficient than that by either DDP isomer, with an unwinding angle calculated at $\phi = 17°$ (compare *cis*-DDP with $\phi = 13°$ and *trans*-DDP with $\phi = 9$–$10°$). In contrast, little unwinding is induced by *cis*-[$PtCl_2$(pyridine)$_2$], with $\phi = 4°$. These results in particular invert the standard cis/trans structure–activity relationships observed previously for [$PtCl_2(NH_3)_2$]. The results are discussed with respect to the previously demonstrated effect of activation of the *trans*-platinum geometry using sterically hindered ligands.

The paradigm for structure–activity relationships of platinum antitumor complexes, exemplified by *cis*-[$PtCl_2(NH_3)_2$],[1] is that only the cis geometry is therapeutically active. The observed inactivity of the trans isomer has had a major influence on both analog synthesis to discover new platinum antitumor agents and the mechanistic interpretation of the antitumor activity of *cis*-DDP. There is general agreement that *cis*-DDP manifests its biological activity through covalent interaction with DNA (Sherman & Lippard, 1987; Reedijk et al., 1987; Farrell, 1989). Possible explanations for the different biological activity of the cis and trans isomers are that cis compounds form platinum–DNA adducts which inhibit DNA replication to a greater extent than those formed from *trans*-DDP (Roberts & Friedlos, 1987; Johnson et al., 1986) and, alternatively, that DNA adducts formed by trans compounds may be repaired more rapidly (Ciccarelli et al., 1985).

The nature of the adducts formed by *cis*- and *trans*-DDP has also been explored to explain the differences in biological activity between the two isomers. *cis*-DDP produces a range of adducts on DNA including monodentate adducts, bidentate adducts such as 1,2-GG or AG, and 1,3-GNG intrastrand cross-links (Sherman & Lippard, 1987; Reedijk et al., 1987). To a lesser extent interstrand GG cross-links (Rahmouni & Leng, 1987) and DNA–protein cross-links are also formed (Zwelling et al., 1979). These lesions result in conformational changes reflected in bending and local unwinding of the DNA and present blocks to DNA polymerases of various origins (Villani et al., 1988; Pinto & Lippard, 1985; Gralla et al., 1987). The interstrand cross-link between two neighboring guanines has also been shown to be a block to RNA polymerase (Lemaire et al., 1991).

Sequencing studies (Pinto & Lippard, 1985) and adduct analysis (Eastman et al., 1988) of DNA modified by *trans*-DDP show a distinct preference for GC sites in comparison to *cis*-DDP. The trans isomer also produces bidentate adducts on DNA, such as a 1,3-GNG intrastrand cross-link, which are presumed to account for its cytotoxicity. The conformational distortions produced by these adducts are dependent on the nature of the intervening base N. The structures of the d(GpTpG) (van der Veer et al., 1986) and d(GpCpG) (Gibson & Lippard, 1987) adducts have been characterized by NMR studies where the intervening C or T base is found to be destacked or "bulged out". The 1,3-GAG binding site within the CCTCGAGTCTCC sequence produces localized disruption of base pairing and destacking of the platinated bases, as indicated from NMR and molecular dynamic modeling studies (Lepre et al., 1990). The 1,3-intrastrand cross-linking by *trans*-[$PtCl_2(NH_3)_2$] also results in bending of the DNA, interpreted in terms of both formation of flexible hinge joints (Bellon & Lippard, 1990; Bellon et al., 1991) and a more directed bend (Anin & Leng, 1990). The unwinding produced by the 1,3-GTG–*trans*-[$Pt(NH_3)_2$] adduct incorporated into a defined oligonucleotide sequence is significantly less than that produced by the corresponding cis adduct (Bellon et al.,

† This publication was supported in part by Grant Number P30 CA22435 from the National Cancer Institute. Its contents are solely the responsibility of the authors and do not necessarily represent the official views of the National Cancer Institute. This work was also supported by award of the J. Walter Juckett Fellowship for 1991/1992 from The Lake Champlain Cancer Research Organization to N.F.

‡ Department of Chemistry.

§ Department of Pathology.

⊥ The Vermont Cancer Center.

® Abstract published in *Advance ACS Abstracts*, September 1, 1993.

[1] Abbreviations: *cis*-DDP, *cis*-[$PtCl_2(NH_3)_2$], cisplatin, *cis*-diamminedichloroplatinum; *trans*-DDP, *trans*-[$PtCl_2(NH_3)_2$]; py, pyridine; CD, circular dichroism; FAAS, flameless atomic absorption spectroscopy; r_b, the number of bound platinum complexes per nucleotide; CT, calf thymus; SC, supercoiled; OC, open circle; r_b(c) value at which the SC and OC forms of DNA comigrate; A/F number of adducts per fragment; XL, fraction of counts running as an interstrand cross-linked band; XL/F, ratio of interstrand cross-links to total platinum bound; XL/A, ratio of interstrand cross-links per adduct.

0006-2960/93/0432-9632$04.00/0

1991). The reduced efficiency of DNA unwinding by the family of *trans*-DDP adducts in comparison to *cis*-DDP adducts is also seen upon platination of a supercoiled DNA such as pUC19; unwinding angles of 13° and 9° at r_b(c) values of 0.076 and 0.11 have been measured for *cis*- and *trans*-DDP, respectively (Keck & Lippard, 1992). The monofunctional *trans*-DDP–DNA intermediate is longer lived than its *cis*-DDP analog and may react readily with glutathione, preventing closure to the bidentate (toxic) lesion (Eastman & Barry, 1987; Bancroft et al., 1990).

In recent contributions, we have reported that the incorporation of a planar ligand within the general structure *trans*-[$PtCl_2$(L)(L′)] ((i) L = L′ = pyridine or thiazole; (ii) L = quinoline and L′ = substituted sulfoxide R′R″SO, R = Me, R′ = Me, CH_2Ph, Ph; (iii) L = quinoline and L′ = NH_3) greatly enhances the cytotoxicity of the trans structure, such that the cytotoxicity is equivalent to that of the analogous cis isomer and indeed that of *cis*-DDP itself (Farrell et al. 1989, 1992; Van Beusichem & Farrell, 1992). The cytotoxicity of trans complexes containing planar ligands is highlighted by a remarkably low resistance factor in both murine and human tumor cell lines resistant to cisplatin, and the complexes furthermore display a different pattern of cytotoxicity in comparison to cisplatin (Farrell et al., 1992). These results strongly imply a new mechanism of action for these complexes (Farrell et al., 1992). By analogy with the DDP isomers, the inhibition of DNA synthesis by *cis*- and *trans*-[$PtCl_2(py)_2$] implies a role for DNA binding in the mechanism of action (Farrell et al., 1992). The presence of a pyridine or quinoline group may present a different array of altered H-bonding and surface interactions as well as steric effects affecting both the kinetics of DNA binding as well as the structures and stability of the adducts formed.

The breaking of the paradigm for structure–activity relationships of platinum antitumor complexes is of fundamental importance. To explain the greatly enhanced cytotoxicity of the pyridine and quinoline derivatives, it is necessary to examine in detail the DNA binding of the new complexes and place these results in context with those previously elucidated for the DDP isomers. These results will further allow development of strategies for the systematic design of platinum antitumor complexes acting by different mechanisms to the presently used agents, and eventually with a different clinical profile of antitumor activity. This paper reports on the results of a comparison between the DNA binding of *cis*- and *trans*-[$PtCl_2$(amine)$_2$] (amine = NH_3, pyridine) with respect to quantitation of DNA binding, conformational changes, DNA–DNA interstrand cross-linking, and sequence specificity.

EXPERIMENTAL PROCEDURES

Starting Materials and Physical Methods. All platinum complexes were synthesized as previously described (Van Beusichem & Farrell, 1992). UV–vis spectra were collected on a Perkin-Elmer Lambda 4B spectrophotometer. Circular dichroism spectra were recorded on a Jobin-Yvon Autodichrograph Mark V spectrophotometer. Flameless atomic absorption spectroscopy (FAAS) measurements were carried out on a Perkin-Elmer 560 instrument with a graphite furnace.

Calf thymus (CT) DNA was purchased from Sigma and used without further purification. The 5′-terminally ^{32}P-labeled 49-bp oligo(deoxynucleotides) (see below for the sequence) were prepared as described previously (Farrell et al., 1990). Briefly, the duplex was synthesized as two separate oligonucleotides on a Du Pont automatic DNA synthesizer. The two single-strand fragments were then purified by electrophoresis on 12% denaturing polyacrylamide gels. The standard methods were used to label the "top-strand" or "bottom-strand" oligomer on the 5′-end with adenosine 5′-[γ-^{32}P]triphosphate followed by removal of the incorporated counts by Du Pont NENSORB 20 nucleic acid purification cartridge. The labeled oligonucleotide was then annealed to the unlabeled complementary strand. The 5′-labeled duplex DNA fragment was finally purified on a 12% polyacrylamide native gel.

```
5′-GACTACTTGGTACACTGACGCGAGCTCGCGGAAGCTCATTCCAGTGCGC-3′ (top)
3′-CTGATGAACCATGTGACTGCGCTCGAGCGCCTTCGAGTAAGGTCACGCG-5′ (bottom)
   1   5   10   15   20   25   30   35   40   45
```

The plasmid pUC19 was either purchased from BRL or prepared by transformation of the plasmid into DH5a competent cells (*Escherichia coli* strain from BRL), amplification of a clone, and purification by using 5′ - 3′ Inc. DNA purification kits. The prepared supercoiled DNA was identified both by the ratio of UV absorption at wavelengths of 260 and 280 nm and by electrophoresis on 1% agarose gel running with BRL plasmid pUC19. The ratios of A_{260}/A_{280} were found to be between 1.83 and 1.85, indicating little contamination by proteins. Supercoiling was determined by staining the bands on agarose gel with ethidium bromide and visualization by UV transillumination. The plasmid contained greater than 90% negatively supercoiled form by comparison with commercial samples from BRL. T4 DNA polymerase and T4 polynucleotide kinase were obtained from BRL.

Platination of DNA. The values of r_b for the binding were also determined and were used for calculation of the cross-link per adduct ratio in the interstrand cross-link assay. CT DNA (0.02 or 0.05 mg/mL) or pUC19 plasmid DNA (0.023 mg/mL) was incubated with varying concentrations (5–200 μM) of platinum complexes in TE buffer (10 mM Tris–HCl, 0.1 mM EDTA, pH 7.4) for 48 h at 37 °C, followed by addition of 200 mM NaCl to terminate the reactions. Unbound platinum complexes were removed by extensive dialysis against TE buffer at 4 °C. The Pt content of the samples was determined by FAAS by suspending the solutions in 2% nitric acid and heating at 50 °C for 24 h or 70 °C for 1 h to hydrolyze the DNA. The experiments on the time dependence of binding were conducted using 0.9 mL of CT DNA (0.023 mg/mL) and 20 μM Pt compounds in TE buffer at 37 °C. Portions of the reaction solution were withdrawn after the designated period of incubation and added to 200 mM NaCl with immediate chilling on ice. The r_b was calculated as previously described (Farrell et al., 1992).

Interstrand Cross-Link Assay. The experiment was conducted in the same way as described previously (Farrell et al., 1990). Briefly, a mixture (20 μL) of the 5′-terminally-labeled 49-mer oligonucleotides in the presence of CT DNA (0.05 mg/mL) and platinum agents with several different concentrations was incubated in TE buffer at 37 °C. The complex [{*trans*-$PtCl(NH_3)$}$_2$-μ-$NH_2(CH_2)_4NH_2$]Cl_2 (Farrell et al., 1990) and *cis*- and *trans*-DDP were incubated for 1 h while the pyridine complexes were incubated for 48 h. The reactions were terminated by addition of 100 mM NaCl. After heating at 90 °C for 5 min, a mixture of the samples and formamide dyes with equal volume was loaded on 8% polyacrylamide denaturing sequencing gels for electrophoresis. The dried gels were then autoradiographed with Kodak XAR-5 films in the presence of intensifying screens at −70 °C. To quantify the interstrand cross-linked DNA which appeared as the bands migrating more slowly than the singly stranded DNA on the

gel, the radioactivity of all bands was measured by a Betascope 603 blot analyzer (Betagen, Waltham, MA).

Sequence Specificity of Platinum–DNA Adducts. Mapping of DNA lesions induced by platinum complexes in the 49-bp oligonucleotides prepared above was conducted as previously described (Royer-Pokora et al., 1981; Farrell et al., 1990). Briefly, the 5′-terminally-labeled DNA was incubated with 5 μM complex for 48 h at 37 °C. The treated DNA fragment was then digested by the 3′ → 5′ exonuclease activity of T4 DNA polymerase of 10 units in a total volume of 40 μL containing Tris–HCl, 50 mM, KCl, 50 mM, and $MgCl_2$, 10 mM, for 90 min at 37 °C. The reactions were terminated by addition of EDTA to 25 mM, followed by denaturing the enzyme by bringing the sample to 90 °C for 5 min. The bound platinum was removed as $[Pt(CN)_4]^{2-}$ in a reaction with 0.3 M NaCN, pH 8.0, for 3 h at 37 °C or overnight at room temperature. The reaction products were diluted by about 5-fold with a formamide/dye sample buffer and directly loaded onto gels without dialysis. The resulting DNA fragments were identified by comparison with the Maxam–Gilbert products (Maxam & Gilbert, 1980) of the same 5′-end-labeled 49-bp DNA by electrophoresis on 12% polyacrylamide sequencing gels under denaturing conditions. The Maxam–Gilbert sequencing was carried out by using a NEN Du Pont sequencing kit.

Unwinding of Negatively Supercoiled DNA. Unwinding of closed circular supercoiled pUC19 plasmid DNA was monitored by an agarose gel mobility shift assay (Keck & Lippard, 1992). The unwinding angle, ϕ, induced per platinum–DNA adduct was calculated upon the determination of the r_b value corresponding to the complete transformation of the supercoiled to nicked form of the plasmid molecule. Samples of *cis*- and *trans*-$[PtCl_2(py)_2]$ were incubated at 37 °C with 3 μg of pUC19 plasmid for 2 days in the dark while those of *cis*- and *trans*-DDP were incubated for a period varying from 1 to 7 h with the other conditions all the same. All samples were then extensively dialyzed against TE buffer using a BRL 1202 MD microdialysis system at 4 °C in the dark. An aliquot of the dialyzed solutions was subjected to electrophoresis on 1% agarose gels running at 25 °C in the dark with TAE buffer (Tris–acetate/EDTA) with voltages set between 30 and 40 V. The gels were then stained with ethidium bromide, followed by photography on Polaroid 667 film with UV transillumination. The other aliquot was used for the determination of r_b values, calculated on the basis of the DNA concentration (ϵ_{260} = 6600 M^{-1} cm^{-1}) and Pt bound measured by FAAS.

RESULTS

Quantitation of Pt–DNA Binding. Structures for all platinum complexes studied in this work are presented in Figure 1. The $[PtCl_2(py)_2]$ complexes inhibit DNA synthesis as measured by labeled thymidine incorporation, implying an involvement of Pt–DNA binding in the mechanism of action (Farrell et al., 1992). The presence of planar ligands, their relative geometry, and the absence (or diminished number) of any NH bonds capable of hydrogen-bonding are the major differences between the new *trans*-platinum complexes and the isomers of $[PtCl_2(NH_3)_2]$. The DNA binding behavior of the NH_3 and pyridine complexes, as a function of both dose and time, was investigated, Figure 2 and Table I. Complex geometry plays an important role in the DNA binding as evidenced by the increased binding of *cis*-$[PtCl_2(py)_2]$ over the trans isomer. The order of binding affinity to DNA under the present experimental conditions was *trans*-DDP ≫ *cis*-DDP (data not shown) ≫ *cis*-$[PtCl_2(py)_2]$ > *trans*-$[PtCl_2(py)_2]$. In contrast to *cis*-$[PtCl_2(py)_2]$, the binding is more quickly saturated by *trans*-$[PtCl_2(py)_2]$ with both concentration and incubation time. The significantly reduced binding for the pyridine complexes implies that the bulky planar ligand compared to NH_3 may sterically inhibit many types of binding on DNA which are available to *cis*- and *trans*-DDP. The lack of hydrogen-bonding in the pyridine complexes may also contribute to the significantly reduced DNA binding. Comparison of the data for CT and pUC19 plasmid DNA, Table I, shows that significantly less binding of the pyridine complexes occurs on the supercoiled DNA for equivalent doses and incubation times. These differences may reflect different conformational changes induced upon Pt binding.

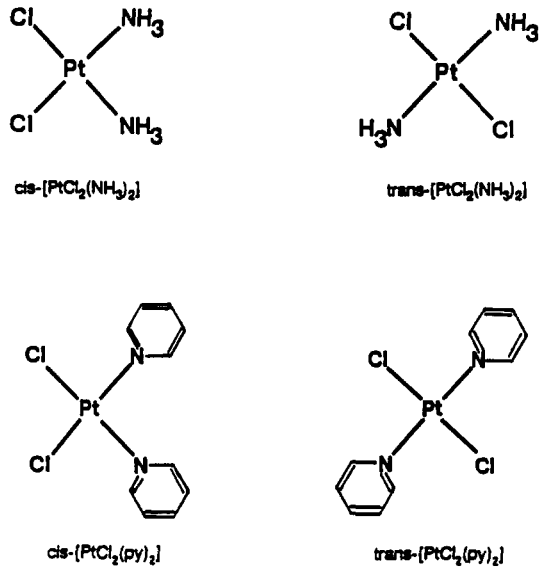

FIGURE 1: Structures of *cis*- and *trans*-$[PtCl_2(amine)_2]$ (amine = NH_3 or pyridine).

Conformational Changes of DNA upon Pt Binding. To understand how the interactions of *cis*- and *trans*-$[PtCl_2(py)_2]$ affect the DNA conformation and how the alteration differs from *cis*- and *trans*-DDP, the platination-induced helical distortions have been monitored by UV/vis and CD spectroscopies, which give information on the overall changes in conformation, and by an electrophoretic gel mobility shift assay which provides information on the DNA unwinding (Keck & Lippard, 1992).

The UV spectrum of DNA modified by *cis*-DDP is characterized by a hyperchromic effect and a slight red shift at the absorption maximum (Horacek & Drobnik, 1971). In contrast, the UV spectrum of DNA platinated by *cis*- and *trans*-$[PtCl_2(py)_2]$ showed also hyperchromicity but with a slight ultraviolet shift. The CD spectra of CT DNA modified by *cis*- and *trans*-$[PtCl_2(py)_2]$ are shown in Figure 3. The major change for *cis*-DDP at low r_b is a slight increase in ellipticity of the positive band with little perturbation of the structure (Johnson et al., 1986). In comparison, Figure 3 displays that although there is little increase in the negative band at 247 nm, the CD spectrum of CT DNA modified by *trans*-$[PtCl_2(py)_2]$ is featured by significant decreases in the positive bands which are now centered at the wavelengths of 221 and 280 nm. Little change is observed with increasing r_b. For *cis*-$[PtCl_2(py)_2]$, the CD spectrum of CT DNA shows a small increase in the positive band with the maximum at 277 nm but an evident decrease at 221 nm with slight red shifts. This behavior is concentration-dependent with a further decrease in the intensity of the band at 221 nm and little

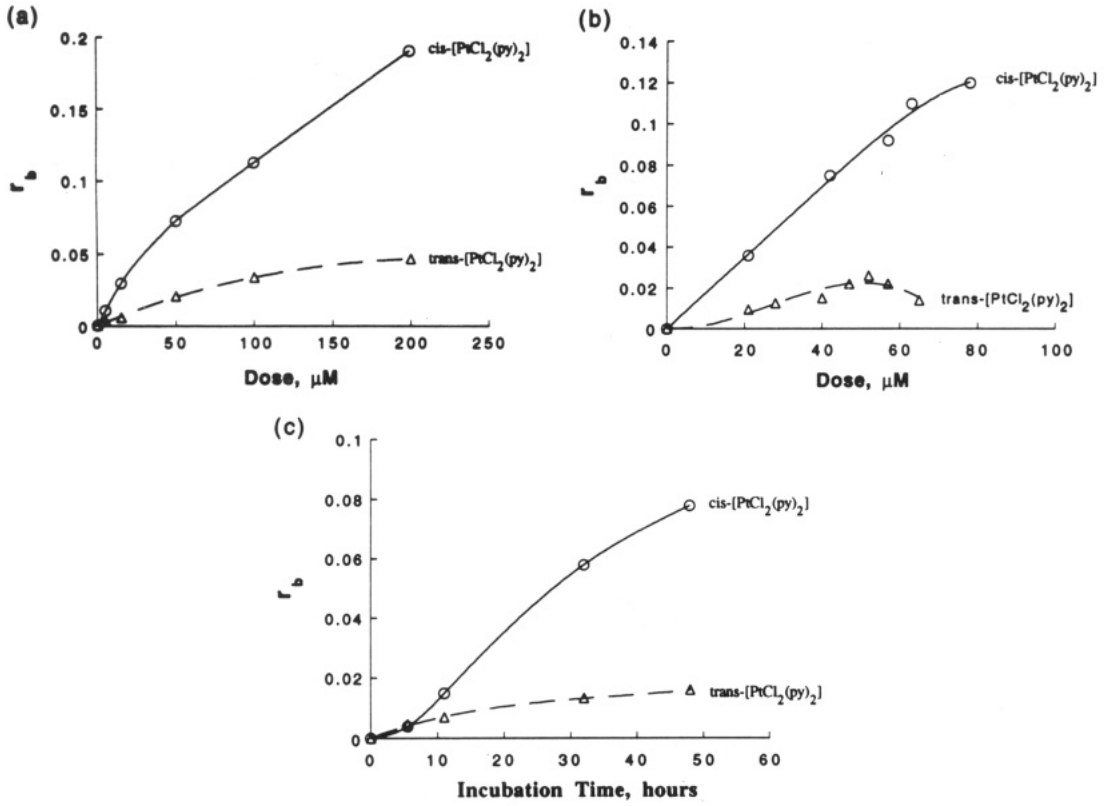

FIGURE 2: Formation of DNA adducts by platinum–pyridine complexes as a function of concentration and time: (a) CT; (b) pUC19; (c) CT. See Experimental Procedures for details.

Table I: Platination of DNA (Calf Thymus and pUC19) by *cis*- and *trans*-$[PtCl_2(py)_2]$[a]

	calf thymus DNA				pUC19 plasmid	
complex	dose (μM)[b]	r_b	time (h)[c]	r_b	dose (μM)[b]	r_b[d]
cis-$[PtCl_2(py)_2]$	5	0.011	5.5	0.004	21	0.036
	15	0.030	11	0.015	42	0.075
	50	0.070	32	0.058	57	0.092
	100	0.113	48	0.078	63	0.11
	200	0.191			78	0.12
trans-$[PtCl_2(py)_2]$	5	0.003	5.5	0.004	21	0.010
	15	0.008	11	0.007	28	0.013
	50	0.026	32	0.013	40	0.015
	100	0.035	48	0.016	47	0.022
	200	0.047			52	0.026
					57	0.022
					65	0.014

[a] Determined as described in the Experimental Procedures. [b] With incubation time of 48 h. [c] With dose of 21 μM. [d] Mean of two and three experiments for *cis*- and *trans*-$[PtCl_2(py)_2]$ complexes, respectively.

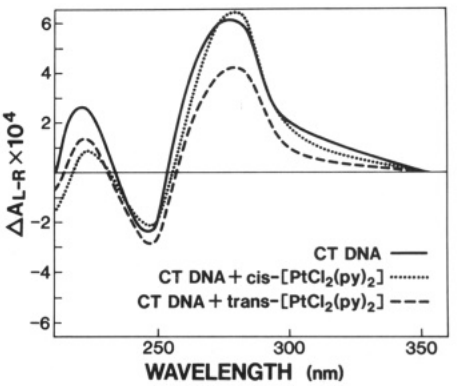

FIGURE 3: Circular dichroism spectra of calf thymus DNA modified by *cis*- and *trans*-$[PtCl_2(py)_2]$ complexes to an equal r_b value of 0.03.

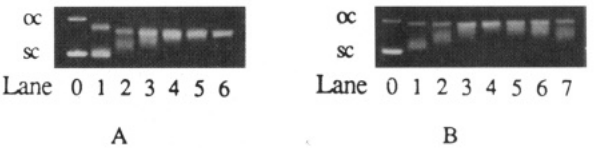

FIGURE 4: Unwinding of supercoiled pUC19 plasmid DNA by *cis*- and *trans*-$[PtCl_2(py)_2]$ (panels A and B, respectively); see also Table II. OC represents the form of nicked plasmid and SC denotes that of circular closed negatively supercoiled plasmid. In panel A, the plasmid was incubated with *cis*-$[PtCl_2(py)_2]$ with the r_b values of 0, 0.054, 0.11, 0.13, 0.15, 0.16, and 0.37 (lanes 0–6, respectively). In panel B, *trans*-$[PtCl_2(py)_2]$ was studied in the same way with r_b values of 0, 0.008, 0.013, 0.014, 0.033, 0.026, 0.026, and 0.012 (lanes 0–7, respectively). The coalescence point where the two forms of DNA (supercoiled and relaxed) comigrate corresponds to $r_b = 0.16$, lane 5, panel A, and $r_b = 0.033$, lane 4, panel B.

change in the 277-nm band (data not shown). This behavior is quite similar to that of DNA modified by *cis*-DDP, suggesting a similar formation of intrastrand cross-links in the total array of adducts made by *cis*-$[PtCl_2(py)_2]$.

In this study, high resolution agarose gel electrophoresis was used to determine the unwinding induced by *cis*- and *trans*-$[PtCl_2(py)_2]$ by monitoring the topological changes of supercoiled plasmid pUC19 DNA, Figure 4. The plasmid was first treated with platinum complexes at varying r_b. For comparison between compounds, the unwinding angle, ϕ, induced per platinum–DNA adduct was calculated by the change in supercoiled topoisomers versus the number of Pt–DNA adducts formed per plasmid molecule, Table II.

Figure 4 shows the decrease in supercoiled (SC) DNA and the appearance of relaxed (OC) DNA as a function of the Pt dose for both *cis*- and *trans*-$[PtCl_2(py)_2]$ (A and B, respectively). *cis*- and *trans*-DDP behaved identically to those in previous reports (Keck & Lippard, 1992). The lower r_b(c) values obtained here are explained by the fact that the present experiments were carried out at 25 °C rather than 4 °C and

Table II: Unwinding of Supercoiled DNA by Platinum Complexes

compound	r_b(c)	unwinding angle (deg)[a]
cis-[$PtCl_2(py)_2$]	0.156	4
trans-DDP	0.053	9–10
cis-DDP	0.043	13
trans-[$PtCl_2(py)_2$]	0.033	17

[a] The unwinding angle is given by $\phi = 18\sigma/r_b(c)$ where $r_b(c)$ is the value at which the two forms of DNA (supercoiled and relaxed) comigrate. Following the analysis of Keck and Lippard (1992), an unwinding angle of 13° for *cis*-DDP was used to calculate σ, giving a superhelical density of –0.0308 under the current experimental conditions. The remaining unwinding angles were calculated using this value of σ.

with the pUC19 DNA from different sources. Variation of the temperature, ionic strength (Scovell, 1986; Bauer, 1978), and content of supercoiled form DNA affects the binding parameters. The behavior of *cis*-[$PtCl_2(py)_2$] is very similar to that of both DDP isomers with a change in mobility of the relaxed plasmid. The complex *trans*-[$PtCl_2(py)_2$] does not apparently alter the mobility of the relaxed form, implying that the binding does not shorten or condense the DNA helix (Cohen et al., 1979; Scovell & Collart, 1985). Above the coalescence point supercoiled DNA reappears (lanes 5–7, Panel B, Figure 4). For only *trans*-[$PtCl_2(py)_2$] a unique observation is that at high concentrations there was less Pt binding to DNA, resulting in diminished conversion of the supercoiled to linear form. This binding pattern is quite reproducible and has not to our knowledge been previously observed for any other Pt complex.

The unwinding angle is given by $\phi = 18\sigma/r_b(c)$ where σ is the supercoil density and $r_b(c)$ is the value at which the two forms of DNA (supercoiled and relaxed) comigrate, Figure 4. Under the present experimental conditions, σ was calculated to be –0.0308 on the basis of the data of *cis*-DDP for which the $r_b(c)$ was determined in this study and $\phi = 13°$ was assumed (Bellon et al., 1991). All unwinding angles for the platinum complexes studied are listed in Table II with the unwinding ability in the order of *trans*-[$PtCl_2(py)_2$] ($\phi = 17°$) > cisplatin (13°) > transplatin (9–10°) > *cis*-[$PtCl_2(py)_2$] (4°). The trans-pyridine isomer is remarkably efficient at unwinding supercoiled DNA. Thus, pyridine substitution results in inversion of the previous cis/trans structure–activity relationship observed for unwinding (Keck & Lippard, 1992).

Interstrand Cross-Link Formation. In this experiment, the 49-bp oligonucleotide was end-labeled and treated with the various platinum agents in the presence of CT DNA. Electrophoresis under denaturing conditions allowed a quantitative assessment of the number of DNA interstrand cross-links formed per DNA adduct (Roberts et al., 1989), Figure 5. As indicated by the control (lane 1) the single-stranded DNA fragment was identified as running fastest on the gel, and the interstrand cross-linked fragment as the double-stranded DNA appeared as the bands migrating more slowly on the gel. As a control, we used the dinuclear interstrand cross-linking agent [{*trans*-$PtCl(NH_3)_2$}$_2$$H_2N(CH_2)_4NH_2$]$Cl_2$ (Farrell et al., 1990) (lane 8). With increasing dose, both *cis*- and *trans*-[$PtCl_2(py)_2$] yielded more interstrand cross-links on DNA but the cross-links induced by the latter appeared to be saturated much more quickly. As a comparison, the binding of 20 μM of *cis*- and *trans*-DDP, corresponding to r_b = 0.01 and 0.02, respectively, showed much less interstrand cross-links than their pyridine derivatives at the same r_b value.

To determine the cross-links per adducts formed [see Roberts et al. (1989)], the radioactivity of all bands was collected and quantified by a Betascope 603 blot analyzer and then used to estimate the fraction of non-cross-linked DNA

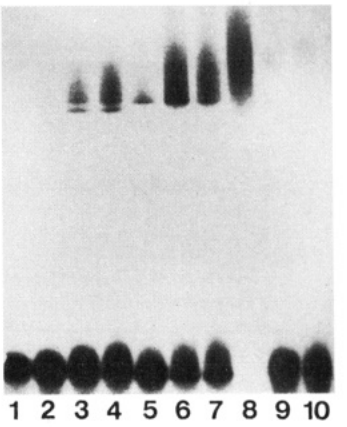

FIGURE 5: DNA–DNA interstrand cross-link formation induced by platinum complexes; see also Table III. The interstrand cross-linked DNA appears as the bands migrating more slowly than the singly stranded DNA on the gel. Lane 1 refers to the control DNA without the treatment with platinum complexes. Lanes 2–4 refer to the DNA fragment treated with *cis*-[$PtCl_2(py)_2$] (1, 5, and 20 μM, respectively). Lanes 5–7 refer to *trans*-[$PtCl_2(py)_2$] (1, 5, and 20 μM, respectively). Lane 8 refers to 1 μM [{*trans*-$PtCl(NH_3)_2$}$_2$$H_2N(CH_2)_4NH_2$]$Cl_2$. Lanes 9 and 10 refer to 20 μM *cis*- and *trans*-DDP, respectively.

for each sample. With an assumption of Poisson distribution, the non-cross-linking fraction in combination with the r_b values and the fragment size was used to calculate the frequency of interstrand cross-linking. As summarized in Table III, *trans*-[$PtCl_2(py)_2$] showed a much higher frequency of interstrand cross-links than *cis*-[$PtCl_2(py)_2$] at the same r_b values, although it had much less reactivity in binding to DNA. The frequency of cross-linking of *cis*-[$PtCl_2(py)_2$] was calculated as similar to that of *cis*-DDP with <5% interstrand cross-links whereas the frequency of interstrand cross-linking for *trans*-[$PtCl_2(py)_2$] is significantly higher than for either *cis*- (Roberts et al., 1989) or *trans*-DDP (data not shown) with between 14% and 23% cross-linked material. For *trans*-[$PtCl_2(py)_2$], the frequency of cross-linking decreases with r_b and was optimized at a dose of less than 10 μM or $r_b < 0.004$. The values for both DDP isomers were <5%, in agreement with previous results (Roberts et al., 1989).

Sequence Specificity of DNA–Pt Adducts. The 5′-^{32}P-labeled sequence-defined 49-bp oligomer as described in the Experimental Procedures was platinated with the pyridine complexes and then used as the substrate for the 3′ → 5′ exonuclease activity of T4 DNA polymerase. The digestion resulted in a pool of shortened fragments of different lengths due to inhibition of the exonuclease activity by the various adducts. Sequencing of these fragments revealed the binding preferences, Figure 6. The assignment of the binding sites is based on the fact that the degraded fragments migrate 0.5–1.5 nucleotides more slowly than the Maxam-Gilbert fragments which identify the modified sites (Malinge et al., 1987). Band intensities are determined by other factors in addition to the population of adducts, and different types of adducts may not inhibit exonuclease activity to the same extent (Malinge et al., 1987). Since r_b varies for the two compounds, direct comparison of sequence preference between the compounds is not valid. However, the relative band intensities *in the same lane* give useful information about the sequence specificity and the relative concentration of adducts for each complex.

cis-[$PtCl_2(py)_2$] (lane 2, Figure 6) produced much fewer stop sites than the trans isomer (lane 3), which may be due to the significant steric effects of its cis-oriented bulky ligands. The major stop sites at G_9G_{10} and $G_{30}G_{31}$ observed for the *cis*-pyridine complex correspond to sites for *cis*-DDP, indi-

Table III: Frequency of Interstrand Cross-Link Formation of *cis*- and *trans*-$[PtCl_2(py)_2]$ Complexes

complex	concn (μM)	r_b[a]	A/F[b]	1 – XL[c]	XL/F[d]	XL/A[e]
cis-$[PtCl_2(py)_2]$	4	0.008 ± 0.001	0.78	0.975	0.025	0.032
	20	0.038 ± 0.004	3.72	0.89	0.12	0.032
	45	0.071 ± 0.011	6.96	0.78	0.25	0.036
trans-$[PtCl_2(py)_2]$	10	0.004 ± 0.001	0.39	0.915	0.089	0.23
	50	0.022 ± 0.006	2.16	0.69	0.37	0.17
	100	0.036 ± 0.001	3.53	0.61	0.49	0.14

[a] Mean of at least two experiments ± SD. The r_b values were measured for the interaction of CT DNA (0.05 mg/mL) with either the *cis*- or *trans*-$[PtCl_2(py)_2]$ complex as described in the Experimental Procedures. [b] Number of adducts per fragment. [c] Mean of two experiments, where XL = the fraction of counts running as the cross-link band. [d] Ratio of interstrand cross-links to total platinum bound, calculated as described previously (Roberts et al., 1989; Farrell et al., 1990). [e] Number of interstrand cross-links per adduct.

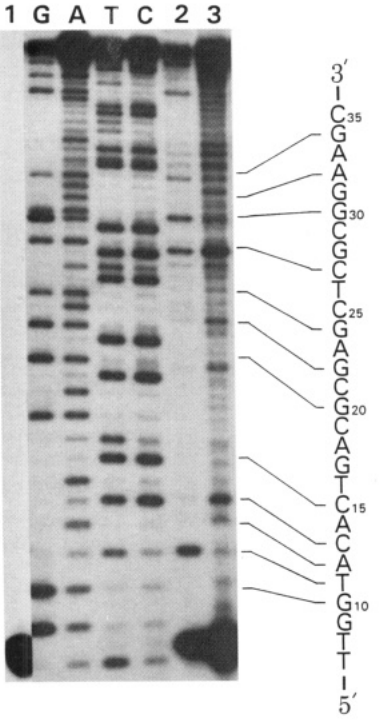

FIGURE 6: Sequence specificity of platinum complex binding to DNA. See the Experimental Procedures for details. Lane 1 represents the unplatinated DNA treated with the exonuclease. 2 and 3 refer to the DNA platinated by 5 μM *cis*-$[PtCl_2(py)_2]$ and *trans*-$[PtCl_2(py)_2]$, respectively, and treated with the exonuclease. Lanes G, A, T, and C were loaded with Maxam–Gilbert sequencing products of G, A + G, T + C, and C reactions, respectively.

cating similar binding modes for both cis compounds (Farrell et al., 1990). In contrast, *trans*-$[PtCl_2(py)_2]$ shows unique stop sites corresponding to platination within the C_{19}–G_{22} sequence. This alternating purine–pyrimidine sequence would be expected to be a good source of interstrand cross-links. This point is further indicated by the presence of a cluster of stop sites corresponding to adducts in a second alternating purine–pyrimidine sequence of C_{27}–G_{30}. The pattern of binding is distinct from those of *cis*-DDP and *cis*-$[PtCl_2(py)_2]$.

DISCUSSION

The purpose of this study was to examine the effect on DNA binding properties upon substitution of a pyridine ligand for NH_3 in the structure $[PtCl_2(amine)_2]$. The *trans*-pyridine complex may be considered a prototype for the class of biologically active *trans*-platinum complexes containing sterically hindered planar ligands (Farrell et al., 1992). The results presented here show that pyridine substitution, especially in the trans geometry, results in greatly increased DNA–DNA interstrand cross-linking and conformational changes as represented by significantly enhanced unwinding of supercoiled DNA. The sequence specificity is further radically different from that of the NH_3 complexes with enhanced affinity for alternating purine–pyrimidine (GC) sequences. These "global" results imply differences in the nature of the adducts formed in comparison to those of $[PtCl_2(NH_3)_2]$. Clearly, all these factors may contribute to the enhanced cytotoxicity of *trans*-$[PtCl_2(py)_2]$.

The DNA binding of *cis*- and *trans*-$[PtCl_2(py)_2]$ to CT DNA has previously been measured and shown to be 5–10 times less than that of the correponding NH_3 complexes (Farrell et al., 1992). The results presented here confirm and extend the earlier ones and show that Pt bound (r_b) increases with both dose and time of incubation. Under the present conditions, less of the trans isomer is bound for any given concentration and the r_b does not significantly increase with long (>10 h) incubation times. The binding of the cis isomer proceeds in an essentially linear fashion, Figure 2. The observed DNA binding of the pyridine isomers confirms that the presence of NH bonds is *not* a prerequisite for Pt–DNA binding, albeit DNA binding is much reduced in the absence of possible H-bonding.

The effects of pyridine substitution are more dramatically observed in the enhanced interstrand cross-linking of the pyridine derivatives. The increased interstrand cross-linking could be of relevance in the collateral sensitivity of the new *trans*-platinum complexes in cisplatin-sensitive and -resistant cells (Farrell et al., 1992). The relationship of gene-specific formation and repair of Pt–DNA lesions is one which is gaining increasing importance with respect to *cis*-DDP resistance (Bohr, 1991). Acquired cellular resistance has been linked to gene-specific repair of the *cis*-DDP interstrand cross-link (Zhen et al., 1992; Jones et al., 1991). Interstrand cross-links could persist even in *cis*-DDP-resistant cells due to a higher proportion of interstrand cross-links, or the formation of cross-links structurally different from those of cis-DDP.

Substitution of a planar ligand such as pyridine for NH_3 dramatically affects the ability of Pt complexes to unwind DNA. Unlike the NH_3 complexes, *trans*-$[PtCl_2(py)_2]$ is now significantly more effective than its cis isomer and, indeed, is the most efficient complex in this study. This efficient and unexpected unwinding may explain in part the greatly increased cytotoxicity of this derivative. Unwinding of DNA could be an important structural motif in recognition of damaged DNA by repair enzymes (Van Houten, 1990; Bellon et al., 1991). In this case, the recognition of a new structural type—trans-planar ligand—with unwinding efficiency equivalent to that of *cis*-DDP is significant. The excision of site-specific Pt–DNA adducts by the UvrABC repair complex is dependent on the exact structure of the adduct (Page et al., 1990). The rates of repair of 1,2-intrastrand GG and AG adducts of $[PtCl_2(en)]$ are generally less than those of the corresponding 1,3-GTG adduct. It is reasonable to assume at this time that the unique binding modes of *trans*-$[PtCl_2(py)_2]$

reflected in the enhanced interstrand cross-linking and large unwinding angle may also lead to differential repair in biological systems. Interestingly, the global array of adducts induced by *trans*-DDP are not efficiently recognized by UvrABC (Beck et al., 1985) whereas those induced by *trans*-$[PtCl_2(py)_2]$ are in fact recognized (Y. Zou et al., unpublished results).

The purpose of this study was to examine the general effects on Pt–DNA binding upon substitution of NH_3 by pyridine. A structural explanation for the observed differences must take into account two major features: (a) the increased importance of surface interactions due to both the presence of planar rings and the absence of H-bonding interactions and (b) the possibility of intercalation or base stacking of the planar rings with adjacent purines and pyrimidines. Further questions arising from this work are the nature of the preferred binding sites on the purines and pyrimidines and the relative rates of monofunctional and bifunctional Pt–base binding in the new complexes. Base binding may not necessarily occur through the "classic" guanine or adenine N7 sites, but exocyclic amines such as the cytidine C4 become sterically possible binding sites. The absence of favorable H-bonding interactions with the guanine C6 carbonyl groups may allow for an altered preference of binding sites on the nucleic acid bases (Marzilli & Kistenmacher, 1977; Farrell, 1980). Indeed, surface interactions may favor minor groove binding over the common major groove sites. These results may then indicate approaches to selective minor groove binding of Pt complexes.

In summary, the use of sterically hindered planar ligands such as pyridine is an important general structural feature capable of systematic modification to produce distinct conformational changes on DNA. These features do not follow the same empirical structure–activity relationships delineated for Pt–NH_3 complexes. Important features for biological activity such as interstrand cross-linking and DNA unwinding are enhanced in the presence of the pyridine ligand with profound consequences for complexes of the trans geometry. The generality of these results for other classes of active *trans*-platinum complexes (Coluccia et al., 1993) and the exact description of the DNA binding modes, especially with respect to identification of the Pt-binding sites on the purine and pyrimidine rings, is under investigation. Finally, these results indicate approaches to systematic design of biologically active Pt complexes complementary to the presently used clinical agents.

ACKNOWLEDGMENT

We thank Marijo Doedee (nee Van Beusichem) for a gift of Pt complexes. We thank the reviewers for constructive comments.

REFERENCES

Anin, M.-F., & Leng. M. (1990) *Nucleic Acids Res. 18*, 4395.
Bancroft D. P., Lepre C. A., & Lippard S. J. (1990) *J. Am. Chem. Soc. 112*, 6860.
Bauer, W. R. (1978) *Annu. Rev. Biophys. Bioeng. 7*, 287.
Beck, D. J., Popoff, S., Sancar, A., & Rupp, W. D. (1985) *Nucleic Acids Res. 13*, 7395.
Bellon, S. F., & Lippard, S. J. (1990) *Biophys. Chem. 35*, 179.
Bellon, S. F., Coleman, J. H., & Lippard, S. J. (1991) *Biochemistry 30*, 8026.
Bohr, V. A. (1991) *Carcinogenesis 12*, 1983.
Ciccarelli R. B., Solomon M. J., Varshavsky A., & Lippard S. J. (1985) *Biochemistry 24*, 7533.
Cohen, G. L., Bauer, W. R., Barton, J. K., & Lippard, S. J. (1979) *Science 203*, 1014.
Coluccia, M., Nassi, A., Loseto, F., Boccarelli, A., Mariggio, M. A., Giordano, D., Intini, F. P., Caputo, P., & Natile, G. (1993) *J. Med. Chem. 36*, 510.
Eastman, A., & Barry, M. A. (1987) *Biochemistry 26*, 3303.
Eastman, A., Jennerwein, M. M., & Nagel, D. L. (1988) *Chem. Biol. Interact. 67*, 71.
Farrell, N. (1989) Transition Metal Complexes as Drugs and Chemotherapeutic Agents, in *Catalysis by Metal Complexes* (James, B. R., & Ugo, R., Eds.) pp 46–66, Reidel-Kluwer, Dordrecht, The Netherlands.
Farrell, N. (1980) *J. Chem. Soc., Chem. Commun.*, 1014.
Farrell, N., Kelland, L. R., Roberts, J. D., & Van Beusichem, M. (1992) *Cancer Res. 52*, 5065.
Farrell, N., Qu, Y., Feng, L., & Van Houten, B. (1990) *Biochemistry 29*, 9522.
Gibson D., & Lippard S. J. (1987) *Inorg. Chem. 26*, 2275.
Gralla, J. D., Sasse-Dwight, S., & Poljak, L. G. (1987) *Cancer Res. 47*, 5092.
Horacek, P., & Drobnik, J. (1971) *Biochim. Biophys. Acta 254*, 341.
Johnson, N. P., Lapetoule, P., Razaka, H., & Villani, G. (1986) in *Biochemical Mechanisms of Platinum Antitumor Drugs* (McBrien, D. C. H., & Slater, T., Eds.) pp 1–28, IRL Press, Oxford.
Jones, J. C., Zhen, W., Reed, E., Parker, R. J., Sancar, A., & Bohr, V. A. (1991) *J. Biol. Chem. 266*, 7101.
Keck, M. V., & Lippard, S. J. (1992) *J. Am. Chem. Soc. 114*, 3386.
Lemaire, M.-A., Schwartz, A., Rahmouni, A., & Leng, M. (1991) *Proc. Natl. Acad. Sci. U.S.A. 88*, 1982.
Lepre, C. A., Chassot, L., Costello, C. E., & Lippard, S. J. (1990) *Biochemistry 29*, 811.
Malinge, J-M., Schwartz, A., & Leng M. (1987) *Nucleic Acids Res. 15*, 1779.
Marzilli, L. G., & Kistenmacher, T. J. (1977) *Acc. Chem. Res. 10*, 146.
Maxam, A. M., & Gilbert, W. (1980) *Methods Enzymol. 65*, 499.
Page, J. D., Husain, I., Sancar, A., & Chaney, S. G. (1990) *Biochemistry 29*, 1016.
Pinto, A. L., & Lippard, S. J. (1985) *Proc. Natl. Acad. Sci. U.S.A. 82*, 4616.
Rahmouni, A., & Leng, M., (1987) *Biochemistry 26*, 7229.
Reedijk, J., Fichtinger-Schepman, A. M. J, van Oosterom, A. T., & van de Putte, P. (1987) *Struct. Bonding (Berlin) 67*, 53.
Roberts, J. D., van Houten, B., Qu, Y., & Farrell, N. (1989) *Nucleic Acids Res. 17*, 9719.
Roberts J. J., & Friedlos, F. (1987) *Cancer Res. 47*, 31.
Royer-Pokora, B., Gordon, L. K., & Haseltine, W. A. (1981) *Nucleic Acids Res. 9*, 4595.
Scovell, W. M., & Collart, F. (1985) *Nucleic Acids Res. 13*, 2881.
Seeman, N. C., Day, R. O., & Rich A. (1975) *Nature 253*, 324.
Sherman, S. E., & Lippard, S. J. (1987) *Chem. Rev. 87*, 1153.
Van Beusichem, M., & Farrell, N. (1992) *Inorg. Chem. 31*, 634.
van der Veer, J. L., Ligtvoet, G. J., van den Elst, H., van der Marel, G. A., & Reedijk, J. (1986) *J. Am. Chem. Soc. 108*, 3860.
Van Houten, B. (1990) *Microbiol. Rev. 54*, 18.
Villani, G., Hubscher, U., & Butour, J.-L. (1988) *Nucleic Acids Res. 16*, 4407.
Zhen, W., Link, C. J., Jr., O'Connor, P. M., Reed, E., Parker, R., Howell, S. B., & Bohr, V. A. (1992) *Mol. Cell Biol. 12*, 3689.
Zwelling, L. A., Anderson, T., & Kohn, K. W. (1979) *Cancer Res. 39*, 365.